FUS interacts with ATP synthase beta subunit and induces mitochondrial unfolded protein response in cellular and animal models

Jianwen Deng[1, #], Peng Wang[1,2, #], Xiaoping Chen[3], Haipeng Cheng[3], Jianghong Liu[1], Kazuo Fushimi[3], Li Zhu [1,*] and Jane Y. Wu [1,3, *]

SI Appendix

Additional notes and discussion

Spectrum of FUS Proteinopathy: FUS proteinopathy is a spectrum of heterogeneous neurodegenerative diseases characterized neuropathologically by inclusion bodies containing the FUS protein. FUS proteinopathy includes frontotemporal lobar degeneration (FTLD) and amyotrophic lateral sclerosis (ALS), and less frequently Basophilic Inclusion Body Disease (BIBD) as well as Neuronal intermediate filament inclusion disease (NIFID) (1). Increased FUS expression has been reported in ALS-FUS and FTLD-FUS patients (2, 3), whereas more than 30 mutations have been identified among ALS-FUS patients (reviewed in (1, 4)). FUS proteinopathy is clinically and genetically heterogeneous.

Suitability of FUS overexpression as a disease model: Recent studies suggest that both loss-of-function and gain-of-function mechanisms may contribute to the pathogenesis of FUS proteinopathy (3, 5-7). Consistent with the observations of increased FUS protein levels in the tissue samples of FUS proteinopathy patients (3, 6, 7), mutations in the 3'-untranslated region (3'-UTR) of the FUS gene in ALS patients are associated with a marked increase in the wild type (Wt) FUS protein (2). To understand the mechanisms by which increased FUS expression or ALS-mutations, we examined effects of FUS expression in inducible cellular model and transgenic fly models for FUS proteinopathy. Increased expression of Wt FUS protein was used to recapitulate FTLD-FUS or ALS-FUS associated with increased Wt FUS expression, whereas an ALS-mutation (P525L), was used to model ALS-FUS with mutations that disrupt the nuclear localization signal of FUS.

A recent study reported generation of FUSDelta14 knock-in mice by targeting a human ALS-associated frame-shift mutation (FUSp.G466VfsX14) into the mouse FUS locus. The heterozygous FUSDelta14 knock-in mice showed progressive neurodegeneration, with their FUS expression maintained at the physiological level (8). Transcriptome analyses of these mice showed that the expression of a number of mitochondrial-associated genes are altered in these mice during disease initiation, suggesting that mitochondrial damage may represent an early pathological change in FUS proteinopathy, consistent with our data showing FUS-induced mitochondrial dysfunction occurring before any detectable cell death (Fig. 1 and 2; *SI Appendix*, **Fig. S3** and **S4**). In addition to the previous findings of mitochondrial damage in FUS proteinopathy patient samples (3, 9), mitochondrial axonal transport defects have been recently reported in iPSC-derived neurons from FUS proteinopathy patients, without expression of exogenous FUS protein (10, 11). Together, these data strongly support that the mitochondrial impairment that we observed in cellular and animal models as well as in patient samples of FUS proteinopathy is not an artifact of FUS overexpression.

The transient membrane potential hyperpolarization induced by FUS: TMRM signal increases when the mitochondrial membrane potential hyperpolarizes. Net proton efflux out of the matrix into the intermembrane space by the electron transport chain is a hyperpolarizing force, and proton re-entry through either complex V or proton leak channels

is a depolarizing force. Our data show that activities of complexes I-IV do not show significant changes in the time scale we studied, whereas complex V activity is inhibited by FUS expression (Fig. 3). Therefore, it is likely that the transient increase in the TMRM signal is due to the ongoing activity of the electron transport chain without efficient proton influx through complex V because of the suppression of the complex V activity by FUS.

Significance of the FUS-ATP5B interaction. Our data demonstrate that expression of FUS, especially the P525L-mutant, significantly reduced the formation of complex V, suppressed ATP synthase activity), reduced mitochondrial ATP synthesis (**Fig. 3**) and induced neurodegeneration (Fig. 5 and Fig. 7). Further experiments show that FUS expression (especially the P525L-mutant) increased the ATP5B/MT-ATP6 ratio (**Fig. 6E, 6G**) and increased the level of free ATP5B not assembled into the ATP synthase complexes (*SI Appendix* **Fig.S5**). FUS-induced decrease in mitochondrial ATP synthesis, imbalance in nDNA vs mtDNA encoded mitochondrial-complex proteins and accumulation of unassembled complex V components may lead to UPR^{mt} activation; and chronic or excessive UPR^{mt} may result in further neurotoxicity, although we cannot exclude other possible mechanisms for FUS to activate UPR^{mt}. Importantly, overexpression of ATP5B exacerbated (**Fig.7** and *SI Appendix* **Fig.S9C**), whereas down-regulation of ATP5B ameliorated FUS-induced neurodegeneration, demonstrating that FUS-induced neurotoxicity is at least partially mediated by ATP5B (**Fig. 7**). Together, these data support the notion that FUS-ATP5B interaction may disrupt the formation and function of ATP synthase complexes, contributing to the activation of UPR^{mt}.

SI Materials and Methods

Fly strains and antibodies. Fly strains are as follows: UAS-RFP, UAS-Wt-FUS-RFP, and UAS-P525L-FUS-RFP flies were described previously (12). The ATP5B-RNAi#2 (v37812), TRAP1-RNAi (v108300), Hsc70-5-RNAi (v106236) and ClpP-RNAi (v103423) stocks were from the Vienna Drosophila RNAi Center. GMR-Gal4, OK371-Gal4, Actin5C-Gal4/Tubulin-Gal80ts, ATP5B-RNAi#1 (28056) and Lon-RNAi (40162) stocks were obtained from the Bloomington Drosophila Stock Center. The ATP5B OE flies expressing the full-length ATP5B under the UAS promoter were generated using a commercial service (Rainbow Transgenic Flies, Inc) in the W1118 background. UAS-Lon (200767) flies were from the Kyoto Stock Center. UAS-ClpP flies were kindly provided by Dr. Tao Wang. Flies were maintained following standard procedures at 25^{o}C.
The antibodies used were as follows: anti-Prohibitin (Millipore), anti-HSP60 (BD), anti-GAPDH (CWBIO), monoclonal anti-myc (Covance), and antibodies against corresponding proteins from ProteinTech Group Inc: FUS, ATP5B, ATP5A1, ATP5O, ATP5F1, IMMT, TOMM20, CytC, HSPA9, PCNA and beta-Actin. It should be noted that the specificity of all antibodies used in this study has been confirmed by published studies.

Cell cultures and transfection. HEK293-based T-REx^{TM}293 cells (Invitrogen) were transfected with pcDNA4 TO/myc-His plasmids (Invitrogen) expressing either Wt or P525L-mutant FUS. Stable expressing cells were selected as individual clones in zeocin (400 μg/mL). Unless specified otherwise, 0.5 ug/mL tetracycline (Tet) was added to the culture medium to induce FUS expression, and cells were incubated for different period of time at 37°C. Stable FUS-deficient (FUS-KO) HEK293 cells were generated using the

CRISPR-Cas9 method following the published protocol (13). Briefly, oligonucleotides corresponding to a guide RNA specifically against the human FUS gene at exon 1 (TGCGCGGACATGGCCTCAAA) were cloned into the targeting vector pSpCas9n(BB)-2A-Puro (Addgen#62988) to generate the FUS targeting construct. Following transfection of the FUS targeting construct into HEK293 cells, single clones were obtained following selection using 5μg/mL puromycin. Stable FUS-KO clones were obtained following Western blotting to examine FUS expression. Cells were cultured (37^{o}C, 5% CO2) in DMEM (Invitrogen) supplemented with 10% FBS (Invitrogen).

Immuno-electron microscopy (IEM) and EM. For the immuno-EM assay using HEK293 cells, inducible cells expressing Wt or P525L-mutant FUS were harvested at the indicated time points and fixed with 4% PFA and 0.2% glutaraldehyde (pH7.2) in PBS for 3 hours at room temperature. Following rinses and post-fixation processing, gelatin-embedded blocks were prepared in 2.3 M sucrose at 4^{o}C. Ultrathin sections (70-nm) were cut at -120^{o}C using dry diamond knives. Following blocking, the sections were immunostained with monoclonal anti-mouse-FUS antibody (1:100) and anti-mouse IgG antibody (1:25) conjugated to 10 nm-colloidal gold particles as well as with polyclonal anti-rabbit-ATP5B antibody (1:100) and anti-rabbit IgG antibody (1:25) conjugated to 25 nm-colloidal gold particles.

For immuno-EM of brain tissues, de-identified postmortem frontal cortex samples from patients affected by FUS-proteinopathy were fixed with 2% PFA and 0.2% glutaraldehyde for 3 hours at room temperature. Samples were embedded in 6% gelatin. Then immuno-staining was performed as described above.

For EM using HEK293 cells or fly retinal tissues, samples were fixed in a solution with 4% paraformaldehyde, 2.5% glutaraldehyde in PBS, pH 7.4, for 12 hours at 4°C and then in a solution with 1% osmium tetroxide in PBS, pH 7.4, for 2 hours at room temperature. The samples were then dehydrated in a series of ethanol solutions (15-minute washes in 10, 25, 40, 55, 70, 85 and 100% ethanol) and embedded in Spurr's resin. Thin sections (70-nm) were prepared and were examined by transmission EM.

All EM images were obtained using a Tecnai Spirit (120kV) electron microscope.

Mitochondrial purification. Mitochondria were purified following published protocols with minor modifications (3, 14). Briefly, stable FUS-expressing HEK293 cells were suspended in isolation butter [220 mM mannitol, 70mM sucrose, 20mM HEPES (pH 7.2), 1mM EGTA], homogenized with a Glass/Teflon Potter Elvehjem homogenizer (Bellco Glass Inc) and then fractionated by sequential centrifugation. Pellets (the mitochondrial fraction) were washed twice with wash buffer (250 mM sucrose, 50mM HEPES, 1mM EGTA, pH7.4) and were then resuspended in the same buffer. The protein concentration was determined by the BCA protein assay (Pierce).

Fly mitochondria were purified following the published protocol with minor changes (15). Fifty flies were transferred into a glass-teflon dounce homogenizer filled with 500 μL of cold isolation buffer (225mM mannitol, 75mM sucrose, 10mM MOPS and 1mM EDTA, 2.5 mg/mL BSA) and were homogenized on ice for 20 strokes. The homogenate was transferred to a 1.5 ml tube for centrifugation at 300g for 5 minutes at 4 °C. The supernatant was then centrifuged at 6,000g for 10 minutes at 4 °C to enrich for mitochondria. The mitochondrial pellet was washed in 1 ml wash buffer (225 mM mannitol, 75 mM sucrose, 10 mM KCl, 10 mM Tris HCl and 5 mM KH_2PO_4) and was then resuspended in the same buffer.

Mitochondrial purification and measuring activities of mitochondrial complexes. Stable inducible HEK293 cells expressing either the vector control or FUS (Wt- or P525L-mutant) were established as described above. Mitochondria were purified from these cells 16-hr following induction with tetracycline (0.5 or 1ug/mL, unless specified) as in our published study (3). Briefly, mitochondria were collected from the boundary between 23% and 40% percoll of gradient centrifugation. Mitochondrial respiratory chain complex activities were measured following the published protocol (16). Briefly, 10 ug of mitochondria was added to a 100ul reaction mixture, containing 30 mM KPO4 pH7.2, 5mM MgCl2, 2.5 mg/mL BSA, 0.3 mM KCN, 0.13 mM NADH, 2 μg/mL antimycin A and 97.5 μM ubiquinone-1. The complex I specific activity was determined by the subtraction of the nonspecific activity in the presence of rotenone from the total NADH oxidase activity in the absence of rotenone. Complex II activity was measured in a reaction mixture containing 30 mM KPO4 (pH7.2), 5mM MgCl2, 2.5 mg/mL BSA, 0.3 mM KCN, 50 uM DCPIP, 2 μg/mL antimycin A and 65 uM decylubiquinone. The complex II specific activity was determined by subtracting the nonspecific activity in the presence of malonate from the total NADH oxidase activity in the absence of malonate. Complex III and IV activities were measured by the reduction and oxidation of cytochrome C, respectively, as described previously (16).

Mitochondrial ATP synthesis assay. Mitochondrial ATP synthesis was measured using the published protocol with minor modifications (17). Briefly, equal amounts (30μg) of purified mitochondria were incubated with reaction substrates (0.15mM P1, P5-di (adenosine) pentaphosphate; 2mM malate; 2mM pyruvate; 0.1mM ADP) with or without oligomycin at 37^{o}C for 5 minutes. Reactions were stopped by adding boiling stop buffer (100mM Tris-HCl, 4mM EDTA, pH 7.4). An equal amount of CellTiter-Glo®reagent (Promega) was added to measure ATP using a microplate reader. Mitochondrial ATP synthesis was quantified by subtracting the ATP content in the absence of oligomycin from the ATP content of the corresponding group with oligomycin treatment.

Measurement of mitochondrial membrane potential. Mitochondrial membrane potential was measured by staining with tetramethylrhodamine methyl ester (TMRM) (Invitrogen). Stable inducible HEK293 cells expressing either the vector control or FUS (Wt or P525L-mutant) were induced at different time points. Cells were incubated with 20 nM TMRM for 20 minutes at 37℃. Cells were washed three times with PBS and cultured in opti-MEM (without phenol red) with 10% FBS and 5 nM TMRM. Respective TMRM intensity was then measured by FACS (BD FACSCalibur) and analyzed using FlowJo. Data were obtained from 3 independent experiments, and 20,000 cells were examined per group in each experiment.

Cell death detection assay. Cell death was measured using Annexin V-FITC Apoptosis Detection Kit I (BD) according to the manufacturer's instruction. Briefly, cells at different induction time points were detached by Trypsin-EDTA, rinsed in cold PBS and then stained with Annexin V-FITC and propidium iodide (PI) followed by immediate analysis (within 1hour) using flow cytometry (BD FACSCalibur). Data were from 3 independent experiments, and more than 20,000 cells were measured per group in each experiment.

Blue native polyacrylamide gel electrophoresis (BN-PAGE), in-gel ATPase assay and clear native polyacrylamide gel electrophoresis (CN-PAGE). BN-PAGE was performed as previously described (18). Briefly, BN-PAGE Buffer (50 mM NaCl, 50 mM imidazole, 2 mM 6-aminohexanoic, and 1 mM EDTA, pH 7.0) was added to 200μg purified mitochondria. Then 6 μl digitonin was added [20% (w/v)] to solubilize mitochondria for 10 minutes on ice. After centrifugation for 30 minutes at 17,000*g*, supernatants were collected, and 2.66 μl 50% glycerol was added. Next, 0.9 μl of Coomassie dye from a 5% (w/v) Coomassie blue G-250 dye stock was added to the samples before they were loaded on to 4–16% acrylamide gradient gels. After proteins migrated into the gels, the electrophoresis buffer was changed to one without any Coomassie blue. Mitochondrial complex V activity was measured using a previously published in-gel ATPase assay (19). Western blotting analyses were carried out after mitochondrial complexes were transferred to PVDF membranes in transfer buffer (25mM Tris, 192mM Glycine, 10% methanol, 0.1% SDS) as previously reported (20, 21).
CN-PAGE analysis of freshly isolated mitochondria followed by Western blotting was carried out as described previously (22).

Immunoprecipitation. Inducible HEK293 cells stably expressing control, Wt or P525L-mutant FUS were induced by Tet (0.5 ug/mL) for 16 hours. The cells were washed with PBS and lysed for 10 minutes on ice in the RSB (10mM Tris-HCl pH7.4, 10mM NaCl, 25mM EDTA, 0.1% NP-40). Cell lysates were then centrifuged at 2,000 rpm for 10 minutes to separate nuclei from the cytoplasmic lysates. These cytoplasmic lysates were collected with protease inhibitor cocktail added (Roche) and adjusted to final concentrations of 50mM Tris-HCl pH7.4 and 150mM NaCl. The cytoplasmic lysates were then used for immunoprecipitation and Western blotting (WB) with the indicated antibodies.

GST-pull down assay. FUS-GST fusion protein was expressed and purified from E coli, as described previously (3). The open reading frame of the human ATP5B gene was cloned into pET28A vector as ATP5BHis-pET28A (Novagen, Inc) to express ATP5B as a His-Tagged protein, ATP5BHis. The plasmid ATP5BHis-pET28A was transformed into BL21(Rosetta) E. coli (Fisher). ATP5B-His protein was then purified from BL21(Rosetta) bacteria using Ni-NTA-resin (GE Healthcare) following the manufacturer's protocol. The GST pull-down assay was performed as previously described (3). Briefly, purified GST, Wt FUS-GST, or P525L-mutant FUS-GST was incubated with purified ATP5B-His in TNE buffer (10 mM Tris, pH 8.0, 150 mM NaCl, 1 mM EDTA, 1% NP-40) on ice for 1 hour. Then the supernatants were incubated with glutathione 4B Sepharose beads at 4°C for 3 hours. Glutathione beads were then washed extensively with ice-cold TNE buffer, and bound proteins were subjected to SDS-PAGE followed by WB analysis. The RNA-dependence of protein interactions was tested by RNaseA treatment as previously reported (23). Briefly, the purified proteins were treated with 50ug/mL RNaseA for 30 minutes at 37°C. The GST pull-down assay was then performed as described above.

Reverse transcription and quantitative real-time polymerase chain reaction (qRT-PCR). Total RNA was isolated from HEK293 cells or fly heads using TRizol reagent (Invitrogen). cDNA synthesis and qPCR were performed as described (24). Data were normalized and quantified using the $2^{-\Delta\Delta CT}$ method as previously reported (25).
To detect UPR^{mt} in HEK293 cells, the following primers were used with *HPRT1* as a

reference gene:
ATF5 forward 5'-CTGGCTCCCTATGAGGTCCTTG-3' and
reverse 5'-GAGCTGTGAAATCAACTCGCTCAG-3';
HSP60 forward 5'-GATGCTGTGGCCGTTACAATG-3' and
reverse 5'-GTCAATTGACTTTGCAACAGTCACAC-3';
HSPA9 forward 5'-CAAGCGACAGGCTGTCACCAAC-3' and
reverse 5'-CAACCCAGGCATCACCATTGG-3';
LONP1 forward 5'-CATTGCCTTGAACCCTCTC-3' and
reverse 5'-ATGTCGCTCAGGTAGATGG-3';
And, *HPRT1* forward 5'-CTTTGCTGACCTGCTGGATT-3' and
reverse 5'-TCCCCTGTTGACTGGTCATT-3'.

To detect UPR^{mt} in *Drosophila*, the following primers were used with *Actin* as a reference gene:
TRAP1 forward 5'-GCAGCGTTCAATATCACCATTG-3' and
Reverse 5'-GACCTCGTGGTCGGAGTATAAGG-3';
HSP60A forward 5'-CACAGAAAAGTCAAGCGA ACTG-3' and
Reverse 5'-GAAACTGGCAAACGGAACATC-3';
Hsc70-5 forward 5'-AAGTGTCGCTCGAACTGC-3' and
Reverse 5'-GAGGTCAGGAAAGCCACTTC-3';
CG5045 (ClpP) forward 5'-GATCATGCTGAAAACCGCTG -3' and
Reverse 5'-CGTGAGAATATGTCGTAGGCC-3';
Lon forward 5'- GGGTGGTTCATCGCTTTA -3' and
Reverse 5'-GATACTTCGCCCGTCATAG -3';
and, *Actin* forward 5'- GCGTTTTGTACAATTCGTCAGCAACC -3' and
reverse 5'- GCACGCGAAACTGCAGCCAA -3'.

Quantification of fly retinal degeneration. The surface area of the fly eye was measured with Image J using fly eye images taken under a bright-field light microscope. The area with disorganized ommatidia or ommatidial loss was considered as the degenerated area. The percentage of degenerated area was calculated by the ratio of degenerated area to the total area of the fly eye. At least 6 eyes were examined in each group, and 3 independent experiments were performed.

Larval movement assay. The assay was done as described previously (12, 26). Briefly, the larval movement index was measured as the number of peristaltic waves during the period of 2 minutes in the late third instar larvae.

Supplementary Figures.

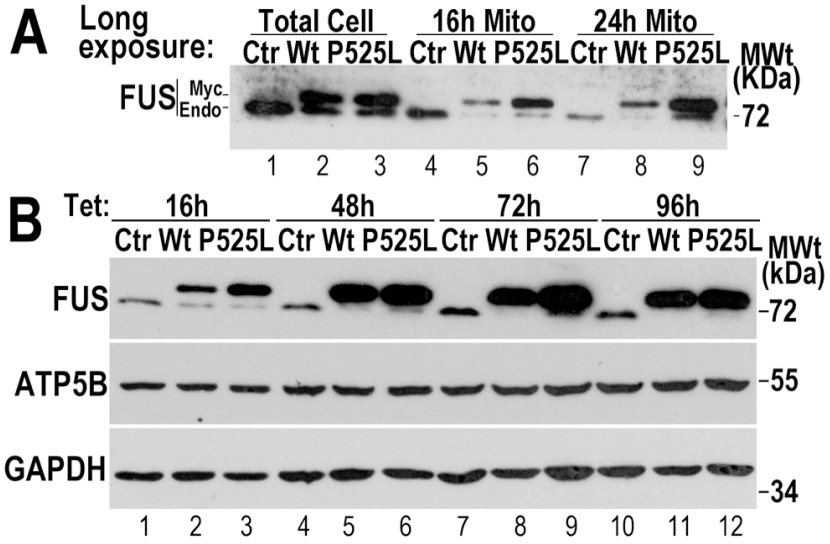

Fig.S1. Protein levels of Wt or P525L-mutant FUS in total cell lysates or purified mitochondria at different time points following FUS induction. (**A**) A longer exposure of the FUS panel in Fig.1B, demonstrating that the endogenous FUS was clearly detected in purified mitochondria, not only from cells expressing either Wt (lanes 5 and 6) or P525L-mutant FUS (lanes 8 and 9) but also from control cells not expressing the exogenous FUS (lanes 4 and 7). (**B**) At corresponding time points to FACS analyses shown in Fig1C and Fig.S2, total cell lysates were also prepared following Tet-induction (1ug/mL) and analyzed by Western blotting using specific antibodies as indicated. Note that this experiment used a higher concentration of tetracycline than that used for Figure 1; thus, the expression levels of FUS were higher than that observed in Figure 1.

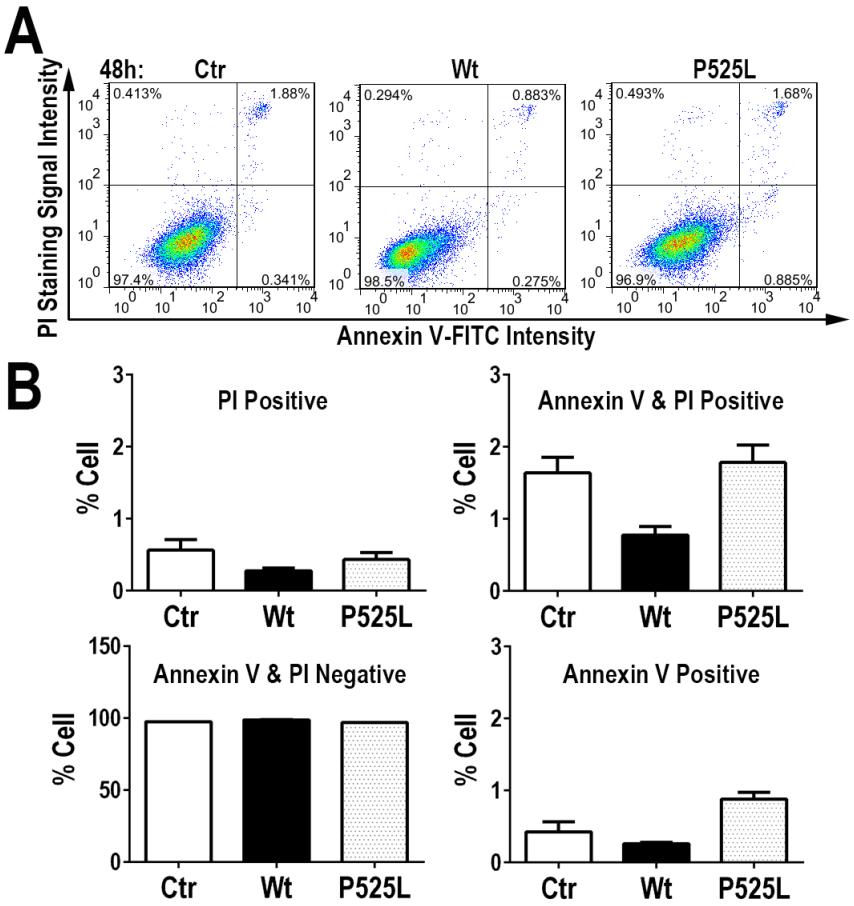

Fig.S2. FUS expression did not cause significant cell death by 48-hr post-induction. (A) Flow cytometry analyses of cells following staining using the Annexin V-FITC/PI kit to quantify cell death in cells expressing Wt or P525L-mutant FUS 48-hr post-induction (0.5 μg/mL tetracycline). (B) Quantification of the percentages of different cell populations. Similar to Fig1D-1G, the quadrant with PI/Annexin V-double negative cells contain healthy cells, the other three quadrants contain dead cells, PI-positive: necroptosis, Annexin V/PI double-positive: late stages of apoptosis or necrosis, and Annexin V-positive and PI-negative: early apoptosis. Data were analyzed using a one-way ANOVA with Bonferroni post hoc test.

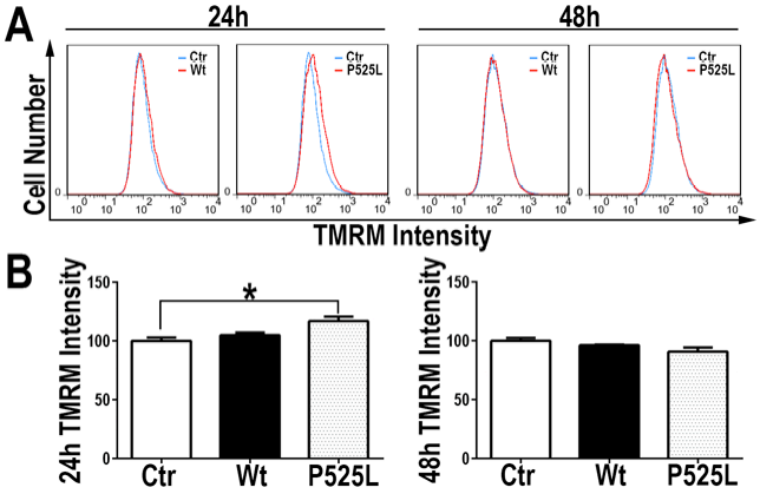

Fig. S3. Expression of P525L-mutant FUS protein led to a transient increase in TMRM signal intensity at an early stage before cell death. (A) FACS analyses following TMRM staining of cells expressing Ctr, Wt- or P525L-mutant FUS protein at 24-hr or 48-hr post-induction (0.5 μg/mL tetracycline). (B) Quantification of TMRM signal intensity. Cells expressing P525L-FUS show increased TMRM intensity as compared with the control group at 24-hr, indicating mitochondrial membrane hyperpolarization. The TMRM signal intensity showed no significant difference between three groups at 48-hrs post induction. Data were analyzed using one-way ANOVA with Bonferroni post hoc test (*: $P<0.05$).

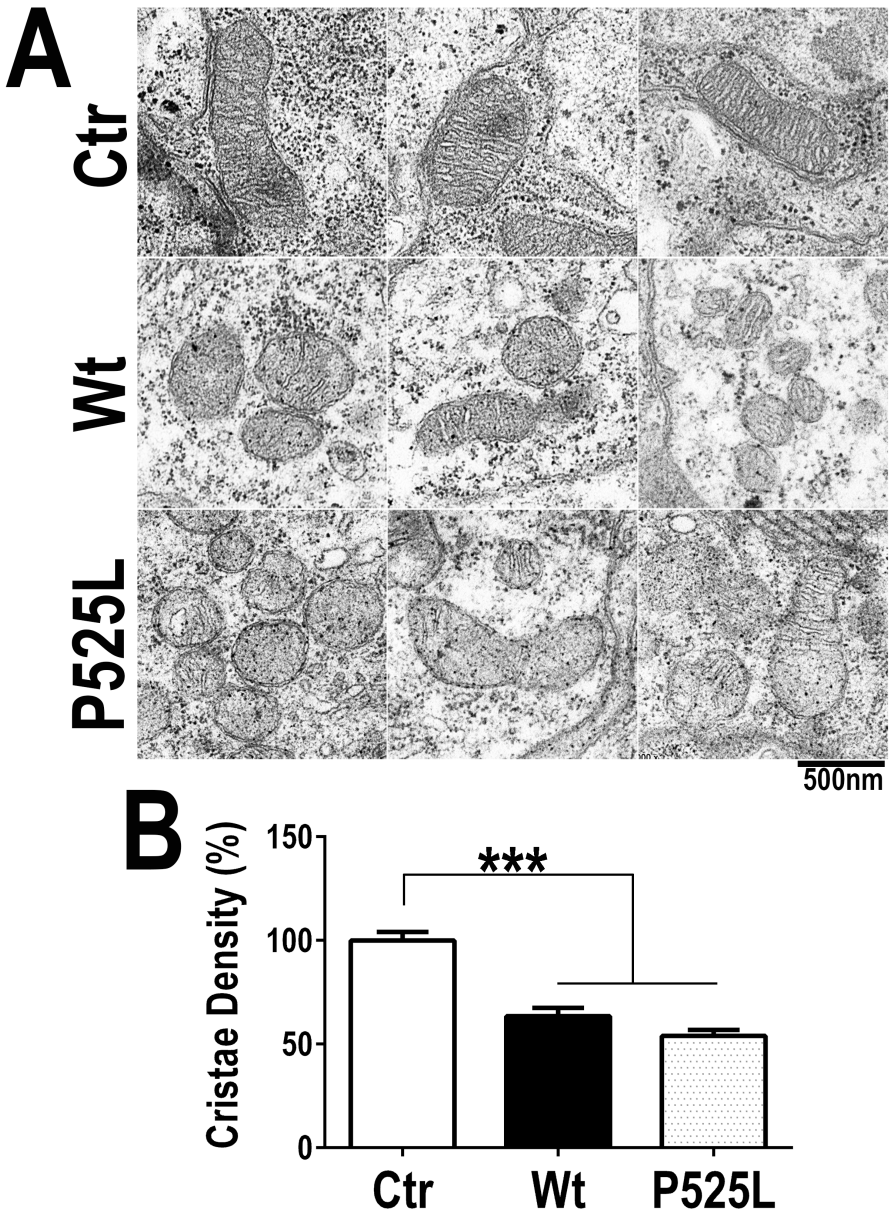

Fig. S4. Mitochondrial cristae loss in flies expressing Wt or P525L-FUS. (**A**) Transmission electron microscopy (TEM) images of fly retinae at adult day 3. (**B**) Mitochondrial cristae density was significantly decreased in flies expressing Wt or P525L-FUS. More than 50 mitochondria per group were quantified. Data were analyzed using a one-way ANOVA with Bonferroni post hoc test (***: $P<0.0001$).

Fly genotypes: **Ctr**: GMR-Gal4/UAS-RFP, **Wt**: GMR-Gal4/UAS-Wt-FUS-RFP, **P525**L: GMR-Gal4/UAS-P525L-FUS-RFP.

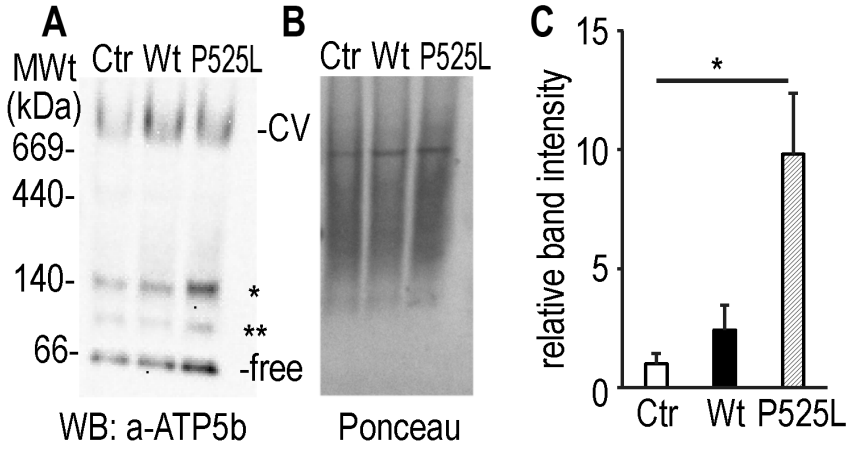

Fig. S5. Clear native polyacrylamide gel electrophoresis (CN-PAGE) analyses of purified mitochondria from cells expressing Ctr, Wt or P525L-mutant FUS at 16-hrs post-induction. (**A**) Western blotting analysis of mitochondrial complex V species, lower molecular weight ATP5B intermediate complexes (marked by "*" and "**") and free ATP5B monomer (marked by "free") using anti-ATP5B antibody. Note that the native gel running time here was short in order to detect the ATP5B monomer; thus, the complex V super-complexes appear smeary and not well-separated. (**B**) Ponceau staining of the membrane in panel A to show that equivalent amounts of total mitochondrial proteins were loaded. (**C**) Quantification of the free ATP5B monomer protein levels in the corresponding groups. Data were analyzed using a one-way ANOVA with Bonferroni post hoc test (*: $P<0.05$; three independent experiments).

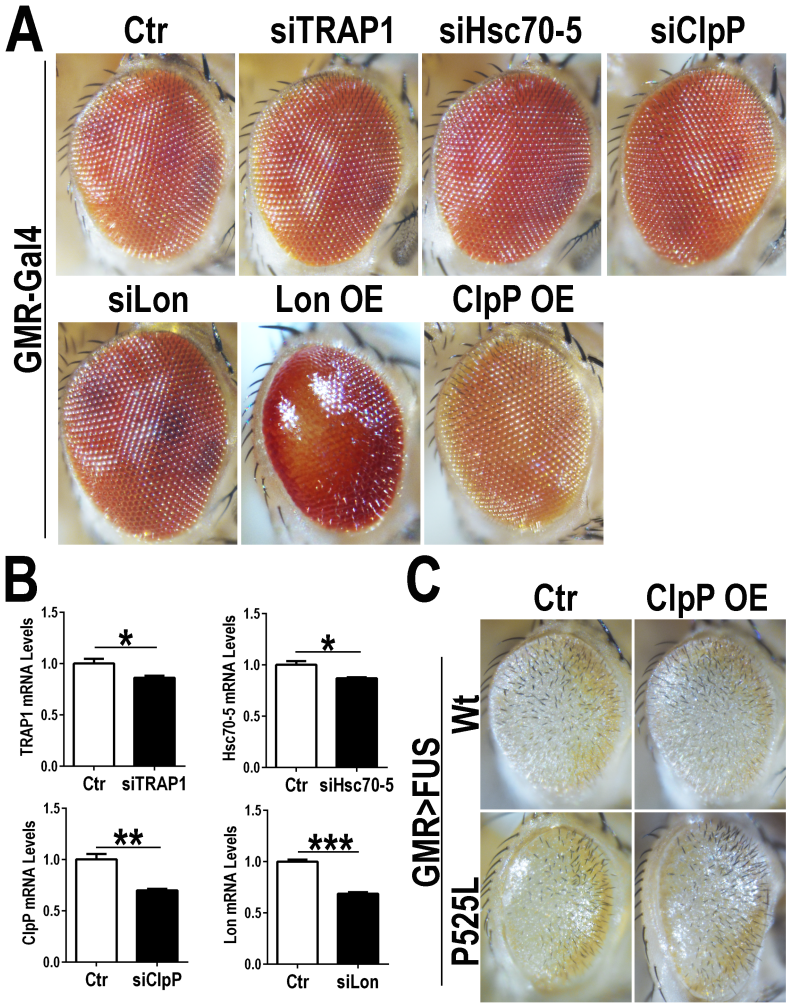

Fig. S6. The retinal morphology of flies expressing control or RNAi against different UPR^{mt} genes and the RNAi efficiency in the corresponding fly lines. (**A**) Microscopic images of fly eyes (5-day old adult) show UPR^{mt} gene RNAi or over-expression under GMR-Gal4 driver expression. Fly genotypes: **Ctr**: GMR-Gal4/UAS-RFP; **siTRAP1**: GMR-Gal4/UAS-siTRAP1; **siHsc70-5**: GMR-Gal4/UAS-siHsc70-5; **siClpP**: GMR-Gal4/UAS-siClpP; **siLon**: GMR-Gal4/UAS-siLon; **Lon OE**: GMR-Gal4/UAS-Lon; **ClpP OE**: GMR-Gal4/UAS-ClpP. (**B**) Quantitative RT-PCR analysis of the mRNA levels of the corresponding UPR^{mt} genes in the fly eyes of different RNAi groups. Data were analyzed using a Student's *t*-test (*: P<0.05; **: P<0.01; ***: P<0.001). (**C**) Microscopic images of fly eyes (5-day old adult) showing that over-expression of ClpP did not affect retinal degeneration in flies expressing Wt or P525L-mumtant FUS. Fly genotypes: **Ctr**: GMR-Gal4/UAS-Wt-FUS-RFP or GMR-Gal4/UAS-P525L-FUS-RFP; **ClpP OE**: GMR-Gal4/UAS-Wt-FUS-RFP/UAS-ClpP or GMR-Gal4/UAS-P525L-FUS-RFP/UAS-ClpP.

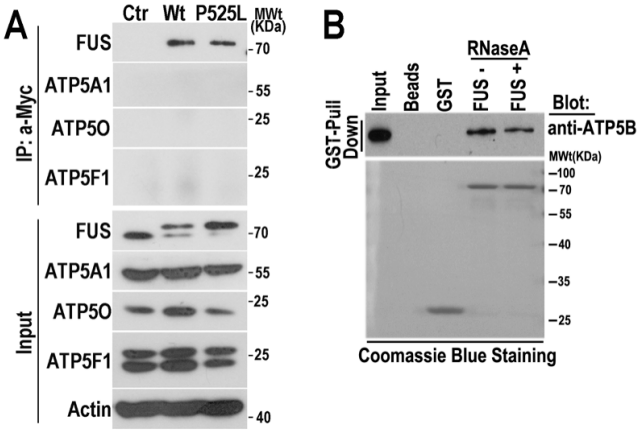

Fig. S7. FUS specifically interacts with ATP5B in an RNA-independent manner. (**A**) Co-immunoprecipitation (co-IP) experiments showed that neither ATP5A1, ATP5O nor ATP5F1 interacted with Wt or P525L-mutant FUS. (**B**) The purified GST tagged Wt FUS and ATP5B-His proteins were treated with RNaseA (50 μg/mL) for 30 minutes at 37°C. GST pull-down assay was performed and bound proteins were analyzed by Western blotting (WB). The lower panel shows a Coomassie blue staining of the GST-tagged proteins used in the assay. It should be noted that only approximately 1/40 of the total input (20ng ATP5B-His) was loaded in the first lane to avoid excessively strong WB signals.

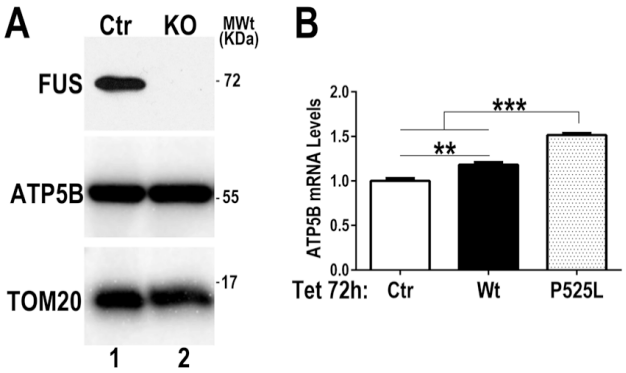

Fig. S8. ATP5B protein levels in control or FUS KO cells and ATP5B mRNA levels in cells expressing Ctr, Wt or P525L-mutant FUS at 72-hr post-induction. (**A**) Western blotting analysis of ATP5B protein levels in Ctr or FUS knock-out (KO) cells, with TOM20 as a loading control. (**B**) Quantitative RT-PCR analysis of ATP5B mRNA levels in cells expressing Ctr, Wt or P525L-mutant FUS at 72-hr post-induction. ATP5B mRNA levels increased significantly in cells expressing Wt or P525L-mutant FUS compared to the Ctr cells. Data were analyzed using a one-way ANOVA with Bonferroni post hoc test (**: $P<0.01$; ***: $P<0.001$; three independent experiments).

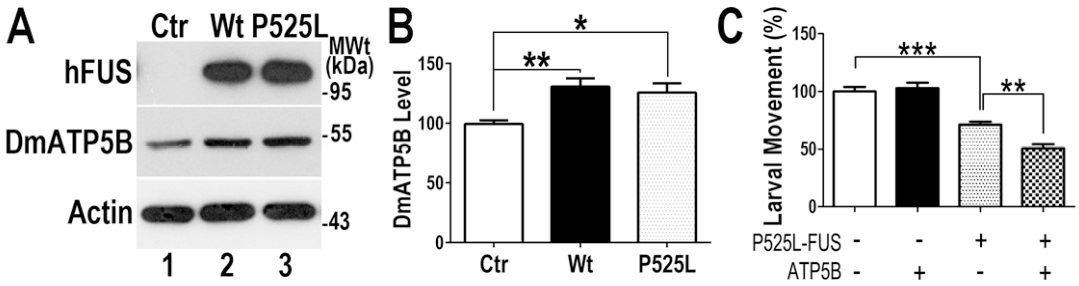

Fig. S9. (A, B) The endogenous DmATP5B protein levels were increased in flies expressing Wt or P525L-FUS. (**A**) Fly eyes expressing Ctr, Wt or P525L-FUS were collected and total lysates were analyzed using Western blotting with the corresponding antibodies as indicated. (**B**) The levels of the *Drosophila* ATP5B protein were significantly increased in day 15 adult flies expressing Wt or P525L-mutant FUS. Fly genotypes: Ctr: GMR-Gal4/UAS-RFP, **Wt**: GMR-Gal4/UAS-Wt-FUS-RFP, **P525L**: GMR-Gal4/UAS-P525L-FUS-RFP. Data were analyzed using a one-way ANOVA with Bonferroni post hoc test (*: $P<0.05$; **: $P<0.01$). (**C**) Over-expression of ATP5B in flies expressing P525L-mutant FUS in motor neurons significantly exacerbated locomotor defects (compare the checkered bar with the gray dotted bar), whereas ATP5B overexpression in control flies did not affect their locomotor activity (compare the black bar with the white control bar). Fly genotypes: **Ctr**: OK371-Gal4/UAS-RFP; **ATP5B**: OK371-Gal4/UAS-ATP5B; **P525L**: OK371-Gal4/UAS-P525L-FUS-RFP; **P525L+ATP5B**: OK371-Gal4/UAS-P525L-FUS-RFP/UAS-ATP5B. Data were analyzed using a one-way ANOVA with Bonferroni post hoc test (**:$P<0.01$; ***: $P<0.001$).

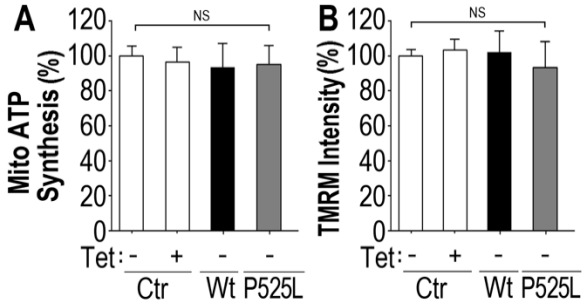

Fig. S10. (A, B) Mitochondrial function was not affected by tetracycline induction in our assays. Vehicle control (90% ethanol, at 1:2000 dilution) or Tet (1ug/mL, from stock of 2mg/mL dissolved in 90% ethanol) was added to the control cells for 24-72 hr. Similarly cultured FUS (Wt or P525L-mutant) stable cells treated with vehicle control without Tet were harvested together with the control cells at 24, 48 and 72 hr for measurement of mitochondrial ATP synthesis and for TMRM staining, as described in Materials and Methods. Western blotting confirmed that there was no induced FUS expression in cells not treated with Tet (also see Fig.1A). No significant changes were detected in mitochondrial ATP synthesis or TMRM staining intensity throughout these time points. Data from 48-hr time were shown, analyzed using ANOVA with Bonferroni post hoc test (3 independent experiments; NS: not significant).

Reference:

1. Mackenzie IRA & Neumann M (2017) Fused in Sarcoma Neuropathology in Neurodegenerative Disease. *Cold Spring Harbor perspectives in medicine* 7(12).
2. Sabatelli M, *et al.* (2013) Mutations in the 3' untranslated region of FUS causing FUS overexpression are associated with amyotrophic lateral sclerosis. *Human molecular genetics* 22(23):4748-4755.
3. Deng J, *et al.* (2015) FUS Interacts with HSP60 to Promote Mitochondrial Damage. *PLoS genetics* 11(9):e1005357.
4. Ratti A & Buratti E (2016) Physiological functions and pathobiology of TDP-43 and FUS/TLS proteins. *Journal of neurochemistry* 138 Suppl 1:95-111.
5. Sun S, *et al.* (2015) ALS-causative mutations in FUS/TLS confer gain and loss of function by altered association with SMN and U1-snRNP. *Nature communications* 6:6171.
6. Sama RRK, *et al.* (2017) ALS-linked FUS exerts a gain of toxic function involving aberrant p38 MAPK activation. *Scientific reports.* 7(1):115. 10.1038/s41598-017-00091-1.
7. Tradewell ML, *et al.* (2012) Arginine methylation by PRMT1 regulates nuclear-cytoplasmic localization and toxicity of FUS/TLS harbouring ALS-linked mutations. *Human molecular genetics* 21(1):136-149.
8. Devoy A, *et al.* (2017) Humanized mutant FUS drives progressive motor neuron degeneration without aggregation in 'FUSDelta14' knockin mice. *Brain : a journal of neurology* 140:2797-2805.
9. Huang EJ, *et al.* (2010) Extensive FUS-immunoreactive pathology in juvenile amyotrophic lateral sclerosis with basophilic inclusions. *Brain pathology* 20(6):1069-1076.
10. Guo W, *et al.* (2017) HDAC6 inhibition reverses axonal transport defects in motor neurons derived from FUS-ALS patients. *Nature communications* 8(1):861.
11. Naumann M, *et al.* (2018) Impaired DNA damage response signaling by FUSNLS mutations leads to neurodegeneration and FUS aggregate formation. *Nature communications* 9.
12. Chen Y, *et al.* (2011) Expression of human FUS protein in Drosophila leads to progressive neurodegeneration. *Protein Cell* 2(6):477-486.
13. Ran FA, *et al.* (2013) Genome engineering using the CRISPR-Cas9 system. *Nature protocols* 8(11):2281-2308.
14. Frezza C, Cipolat S, & Scorrano L (2007) Organelle isolation: functional mitochondria from mouse liver, muscle and cultured fibroblasts. *Nature protocols* 2(2):287-295.
15. Villa-Cuesta E & Rand DM (2015) Preparation of Mitochondrial Enriched Fractions for Metabolic Analysis in Drosophila. *Jove-J Vis Exp* (103).
16. Spinazzi M, Casarin A, Pertegato V, Salviati L, & Angelini C (2012) Assessment of mitochondrial respiratory chain enzymatic activities on tissues and cultured cells. *Nature protocols* 7(6):1235-1246.
17. Manfredi G, Spinazzola A, Checcarelli N, & Naini A (2001) Assay of mitochondrial ATP synthesis in animal cells. *Methods in cell biology* 65:133-145.
18. Wittig I, Braun HP, & Schagger H (2006) Blue native PAGE. *Nature protocols* 1(1):418-428.
19. Krause F, Reifschneider NH, Goto S, & Dencher NA (2005) Active oligomeric ATP synthases in mammalian mitochondria. *Biochem Biophys Res Commun* 329(2):583-590.
20. Garcia CJ, Khajeh J, Coulanges E, Chen EI, & Owusu-Ansah E (2017) Regulation of Mitochondrial Complex I Biogenesis in Drosophila Flight Muscles. *Cell reports* 20(1):264-278.
21. Kim K, Kim SH, Kim J, Kim H, & Yim J (2012) Glutathione S-Transferase Omega 1 Activity Is Sufficient to Suppress Neurodegeneration in a Drosophila Model of Parkinson Disease. *Journal of Biological Chemistry* 287(9):6628-6641.
22. Ohsakaya S, Fujikawa M, Hisabori T, & Yoshida M (2011) Knockdown of DAPIT (Diabetes-associated Protein in Insulin-sensitive Tissue) Results in Loss of ATP Synthase in

Mitochondria. *Journal of Biological Chemistry* 286(23):20292-20296.

23. Liu-Yesucevitz L*, et al.* (2010) Tar DNA binding protein-43 (TDP-43) associates with stress granules: analysis of cultured cells and pathological brain tissue. *PLoS ONE* 5(10):e13250.
24. Fiorese CJ*, et al.* (2016) The Transcription Factor ATF5 Mediates a Mammalian Mitochondrial UPR. *Current biology : CB* 26(15):2037-2043.
25. Livak KJ & Schmittgen TD (2001) Analysis of relative gene expression data using real-time quantitative PCR and the 2(-Delta Delta C(T)) Method. *Methods* 25(4):402-408.
26. Li Y*, et al.* (2010) A Drosophila model for TDP-43 proteinopathy. *Proceedings of the National Academy of Sciences of the United States of America* 107(7):3169-3174.